Differential Effects of HCN Channel Block on On and Off Pathways in the Retina as a Potential Cause for Medication-Induced Phosphene Perception

Sebastian Bemme,[1,2] Michael Weick,[1,2] and Tim Gollisch[1,2]

[1]Department of Ophthalmology, University Medical Center Göttingen, Göttingen, Germany
[2]Bernstein Center for Computational Neuroscience Göttingen, Göttingen, Germany

Correspondence: Tim Gollisch, Department of Ophthalmology, University Medical Center Göttingen, Waldweg 33, 37073 Göttingen, Germany; tim.gollisch@med.uni-goettingen.de.

Submitted: January 27, 2017
Accepted: August 3, 2017

Citation: Bemme S, Weick M, Gollisch T. Differential effects of HCN channel block on On and Off pathways in the retina as a potential cause for medication-induced phosphene perception. *Invest Ophthalmol Vis Sci*. 2017;58:4754–4767. DOI:10.1167/iovs.17-21572

Purpose. Phosphene perception is a characteristic side effect of heart rate–reducing medication that acts on hyperpolarization-activated cyclic nucleotide-gated (HCN) ion channels. It is hypothesized that these phosphenes are caused by blocking HCN channels in photoreceptors and neurons of the retina, yet the underlying changes in visual signal processing in the retina caused by the HCN channel block are still unknown.

Methods. We examined the effects of pharmacologic HCN channel block on the encoding of visual signals in retinal ganglion cells by recording ganglion cell spiking activity from isolated mouse retinas mounted on multielectrode arrays. Spontaneous activity and responses to various visual stimuli were measured before, during, and after administration of 3 μM ivabradine.

Results. Retinal ganglion cells generally showed slower response kinetics and reduced sensitivity to high temporal frequencies under ivabradine. Moreover, ivabradine differentially affected the sensitivity of On and Off ganglion cells. On cells showed reduced response gain, whereas Off cells experienced an increase in response threshold. In line with these differential effects, Off cells, in contrast to On cells, also showed reduced baseline activity during visual stimulation and reduced spontaneous activity. Furthermore, Off cells, but not On cells, showed increased burst-like spiking activity in the presence of ivabradine.

Conclusions. Our data suggest that pharmacologic HCN channel block in the retina leads to a shift in the relative activity of the On and Off pathways of the retina. We hypothesize that this imbalance may underlie the medication-induced perception of phosphenes.

Keywords: phosphenes, HCN channels, pharmacology, ganglion cells, neural coding

Hyperpolarization-activated cyclic nucleotide-gated (HCN) channels are voltage-gated ion channels with the unusual characteristic that they become activated upon hyperpolarization of the cell membrane.[1,2] They are primarily found in the central nervous system and in the heart. The retina, as part of the central nervous system, expresses all four HCN channel isoforms (HCN1–4) that have been identified thus far,[3,4] and HCN1 shows particularly strong expression in the inner segments of retinal photoreceptors, suggesting a role in shaping photoresponses.[5] When photoreceptors hyperpolarize upon illumination, the HCN1 channels mediate a hyperpolarization-activated inward current, known as I_h,[6,7] which counteracts the hyperpolarization and restricts retinal photoreceptor activation.[8–13]

The role of HCN channels in retinal signal processing has in recent years also come into focus from a medical perspective. Because HCN channels in the heart play an important part in generating and modulating the cardiac rhythm,[14] selective HCN channel antagonists are used in heart-rate-reducing pharmaceuticals, such as ivabradine.[15–18] The most common side effect of this medication is the perception of luminous phenomena, so-called phosphenes, which are thought to arise from the block of HCN channels in retinal photoreceptors,[19] although the underlying neuronal signaling is still not fully understood.

Indeed, ivabradine administration suppresses I_h currents in rod photoreceptors in a dose-dependent fashion after repeated stimulation,[20] similar to results obtained in photoreceptors of HCN1 knockout mice.[21] Also, administration of ZD7288, an alternative HCN channel blocker, leads to prolonged hyperpolarization of rods and cones after repeated light flashes.[22] Moreover, systemic administration of ivabradine in rats or mice leads to dose-dependent alterations of ERG b-wave amplitudes during sinusoidal light stimulation showing that the drug, although designed to be blocked by the blood–brain barrier, is nonetheless able to cross the blood–retina barrier and influence the physiology of the retinal network.[21,23] Similar effects on ERG b-waves were also found in HCN1 knockout mice,[5,24] consistent with the action of ivabradine on HCN channels in the retina. From the observed effects of the HCN channel block on photoreceptor signals, phosphene perception is hypothesized to arise because the HCN channel block enlarges rod photoreceptor signals from spontaneous rhodopsin isomerizations and that these enlarged noise signals more easily generate downstream retinal activity.[19] This mechanism, however, is likely most effective in darkness or low light intensities and therefore does not yet explain why phosphenes can occur during or may even be enhanced by visual stimulation.[25,26]

This raises the questions how the pharmacologic blocking of HCN channels affects the processing of visual information in the retinal network under visual stimulation, how it alters the signals communicated to the brain by retinal ganglion cells, the output neurons of the retina, and how these altered signals may underlie the reported perception of phosphenes. We therefore investigate how administration of ivabradine modifies the spiking of retinal ganglion cells under constant and temporally modulated illumination, focusing in particular on comparing changes in the On and Off pathways of the retina.

Methods

Electrophysiologic Recordings

Retinas were obtained from wild-type C57BL/6 mice of either sex. All experimental procedures conformed with German law and institutional guidelines of the University Medical Center Göttingen and adhered to the ARVO Statement for the Use of Animals in Ophthalmic and Vision Research. Prior to isolation of the retina, animals were dark-adapted for at least 30 minutes and then killed by cervical dislocation. Both eyes were removed and dissected under a stereo-microscope equipped with infrared illumination and night vision goggles. Retinas were isolated from the eyecups and stored in oxygenated (95% O_2/5% CO_2) Ames medium (Sigma-Aldrich, Munich, Germany), supplemented with 22 mM $NaHCO_3$ and 6 mM D-glucose. Spikes were recorded by mounting a retina ganglion-cell-side-down onto a multielectrode array (either 60 or 252 electrodes, 10-μm electrode diameter, 60- or 100-μm minimal electrode spacing; Multi Channel Systems, Reutlingen, Germany). During recordings, the retina was constantly perfused with the Ames medium at a flow rate of approximately 4 mL/min and heated to a constant temperature of approximately 31°C. Voltage signals were amplified, band-pass filtered between 300 Hz and 5 kHz, and stored digitally at 10-kHz sampling rate. Spike sorting was performed with a custom-made software program, based on a Gaussian mixture model and an expectation-maximization algorithm.[27]

Administration of Pharmacology

Ivabradine was obtained as caplets (Servier, Munich, Germany). After abrading the coating film with a scalpel, a caplet was pulverized, and the weight was measured with micro scales. The pulverized caplet was dissolved in an appropriate volume of purified water to obtain a solution of 300 μM ivabradine. For experimental application, the solution was further diluted in Ames medium for a final concentration of 3 μM ivabradine. We chose this concentration for comparability with previous investigations of photoreceptors and bipolar cells, where the same concentration had been applied.[20,21] Furthermore, initial exploration with varying concentrations of ivabradine had shown that the applied concentration is sufficient to yield robust effects without affecting the stability of our recordings. All solutions were freshly prepared right before the experiment started. During the experiment, application of ivabradine and washout were controlled by switching between perfusion solutions with and without ivabradine.

Visual Stimulation

Visual stimulation was controlled through custom-made software, based on C++ and the OpenGL library. Stimuli were displayed on a computer-controlled, gamma-corrected white organic light-emitting diode (OLED) display (600 × 800 pixels; eMagin, Bellevue, WA, USA) at 60 Hz refresh rate and projected onto the photoreceptor layer of the retina through a telecentric lens (Edmund Optics, Karlsruhe, Germany) with a pixel size of 7.5 × 7.5 μm on the retina. Mean light intensity was set to 0.6 mW/m^2 in the mesopic range. We estimated the resulting isomerization rates by using the measured spectral distribution of emission by the OLED, the known spectral sensitivity curves of mouse photoreceptors, and collecting areas of 0.5 μm^2 for rods and 0.2 μm^2 for cones,[28] using the values for transverse rather than head-on stimulation because our preparation likely bends photoreceptors slightly sideways. This yielded approximate isomerization rates of 350 isomerizations/s/rod, 150 isomerizations/s/M-cone, and 0.1 isomerizations/s/S-cone, indicating that activation of the retina occurred through a combination of M-cones and rods. For measurements of spontaneous activity, we also performed experiments under photopic conditions by setting the mean light intensity to 77 mW/m^2, corresponding to about 4.5×10^4 isomerizations/s/rod, 1.9×10^4 isomerizations/s/M-cone, and 13 isomerizations/s/S-cone. At these isomerization levels, rod signals are nearly saturated, and retinal signaling is thus strongly dominated by M-cone activation.[29]

Identification of On, Off, and On-Off Ganglion Cells

Recorded ganglion cells were classified into On-type and Off-type based on responses to alternating 800-ms episodes of bright and dark illumination (100% contrast) at the beginning of each experiment. Cells whose average spike rate did not reach 4 Hz during either bright or dark illumination were classified as unreliable and excluded from further analysis, affecting 71 of a total of 722 recorded cells. For all other cells, we calculated the ratio of the average spike count after onset of bright and dark illumination, respectively, each evaluated in the window of 25 to 500 ms after illumination onset. If this ratio was $\geq$2, the cell was classified as an On cell; if the ratio was $\leq$0.5, it was classified as an Off cell. The remaining cells, that is cells with a ratio between 0.5 and 2, were classified as On-Off cells.

Computation of Response Latencies

The alternating bright and dark illumination was also applied to compute response latencies, which we here defined as the time after light onset (for On cells) or light offset (for Off cells) when the firing rate increased most sharply. We constructed peristimulus time histograms (PSTHs) for either the bright illumination (in the case of On cells) or the dark illumination (Off cells) by computing average firing rates in a 20-ms sliding window, shifted along the stimulus duration at a resolution of 1 ms. To find the time where the PSTH increased most strongly, we subtracted from each entry in the PSTH the value at 20 ms earlier and defined the latency as the time point where this difference was maximal. To reduce noise from sparsely responding cells, we excluded cells from this analysis for which this maximal difference value was smaller than 15 Hz, which affected 5 of the 122 cells that were recorded under mesopic light conditions for the detailed analysis of temporal filtering.

Assessment of Temporal Filtering and Sensitivity

To analyze the temporal filtering characteristics and the sensitivity of the recorded ganglion cells with and without pharmacologic HCN channel block, we applied temporal white noise stimulation. New illumination levels of the retina were drawn at 30 Hz from a Gaussian distribution around the mean light intensity. The contrast level of the white noise

Investigative Ophthalmology & Visual Science

stimulus is given by the SD of the Gaussian distribution of light intensity values, which was here set to 30% of the mean light intensity. We used seven runs of the temporal white noise stimulation, each lasting 6 minutes, separated by approximately 2-minute recovery in darkness. Application of ivabradine started after the first run and was washed out after the fourth. The first 30 seconds of each run were discarded to avoid transient effects of adaptation. For analysis, the stimulus was upsampled by a factor of 33 to a temporal resolution of about 1 ms. For each cell and each run, we then computed a temporal filter by reverse correlation of the stimulus $s(t)$, defined as the relative deviations from the mean light intensity, and the response $r(t)$, obtained as the firing rate binned at the same resolution as the stimulus. The reverse correlation yields the "spike-triggered average,"[30] which corresponds to the average stimulus sequence that preceded a spike and can be viewed as the cell's preferred sequence of light intensity. Also, the spike-triggered average can be viewed as a temporal filter that, when applied to the incoming stimulus sequence, can be used to predict the activation level of the cell. In this view, which we also adopt here, the filter is typically displayed as the time-reversed spike-triggered average, so that positive time corresponds to time preceding the occurrence of a spike. Concretely, we computed the reverse correlation in the frequency domain[31] by computing the filter $\tilde{F}(\omega)$ as the product of the complex conjugated Fourier transform of the stimulus, $\tilde{s}^*(\omega)$, and the Fourier transform of the response, $\tilde{r}(\omega)$: $\tilde{F}(\omega) = \tilde{s}^*(\omega)\tilde{r}(\omega)$. The filter $F(t)$ in the time domain was obtained as the inverse Fourier transform of $\tilde{F}(\omega)$. Filters were computed over a temporal window of 1 second, corresponding to 1000 sample points, and were normalized to a fixed Euclidean norm so that the sum of squares of the filter values had a fixed value. Concretely, we set the Euclidean norm to equal the stimulus contrast level of 0.3. This ensures that the filter output stretches over the same range as the stimulus contrast when a white noise signal of unit variance is used as input. Time to peak of the filters was evaluated by finding the time point corresponding to the largest positive (for On cells) or largest negative (for Off cells) value of the filter. Biphasicness was assessed by computing a biphasic index as the positive ratio of the size of the secondary filter peak (in the direction of the nonpreferred stimulus contrast) to the size of the primary filter peak (in the direction of the preferred stimulus contrast).[32,33]

Cells were excluded from further analysis when the polarity of the temporal filters (i.e., On-type or Off-type) was not consistent between the different episodes of temporal white noise stimulation or when the peak size in the temporal filter was smaller than 4 SDs of the filter values (139 of 651 cells recorded under this stimulus paradigm). Furthermore, cells were excluded when classification into On and Off based on alternating bright/dark illumination was not consistent with the shape of the temporal filter (17 further cells).

To assess a neuron's sensitivity under the temporal white noise stimulation, we used the obtained temporal filter to construct a full linear-nonlinear (LN) model by computing a nonlinearity that relates the filter activation to the actual spiking probability of the neuron.[30] To obtain the nonlinearity, we convolved the stimulus sequence with the temporal filter to compute a filter output. We then binned the filter output values into 20 bins so that each bin contained the same number of data points and computed the average filter output, as well as the average number of corresponding measured spikes for each bin. The histograms were fitted by the following sigmoid function:

$$R(x) = \frac{R_{max}}{1 + e^{-4G(x-x_0)/R_{max}}} \quad (1)$$

The shape parameters of the sigmoid, given by the maximal firing rate R_{max}, the gain G, which is also the maximal slope of the sigmoid, and the offset x_0, which is also the inflexion point, were obtained by a least-squares fit. To describe drug-induced shifts of the nonlinearities, we used the setpoint $x_{R=0}$ of the nonlinearity, which is an estimate of the threshold that is obtained by extrapolating the curve's tangent through the inflexion point to $R = 0$: $x_{R=0} = x_0 - R_{max}/2G$. Finally, the baseline activity of the nonlinearity was defined as the spike rate when the filter output equaled zero: $R(x = 0)$.

Analysis of Spontaneous Activity

Spontaneous activity was measured while illuminating the retina with a gray background at the mean light intensity of either 0.6 mW/m^2 (mesopic condition; see Visual Stimulation) or 77 mW/m^2 (photopic condition). Spontaneous activity was recorded for 30 minutes, with drug delivery starting after the first 10 minutes. The 20 minutes in the presence of the drug were divided into six periods of 200 seconds. We counted the number of spikes for each 200-second time period, subtracted the number of spikes from the last 200-second time period before drug delivery, and normalized by the sum of these two spike counts to obtain the relative change in spontaneous activity. In this set of experiments, we also recorded responses to alternating dark and bright illumination for 2 minutes and to temporal white noise stimulation for 6 minutes. These measurements were taken before and after measuring spontaneous activity as well as after washout.

Quantification of Spike-Burst Firing

Some cells appeared to change their spontaneous firing patterns from Poisson-like activity to burst firing after application of ivabradine. To quantify these changes, we calculated for each 200-second episode of spontaneous activity a burst index (BI), as described by Jones et al.,[34] which relates the total time of long interspike intervals (ISIs) to the total recording time and the duration of long ISIs to the mean ISI. The set of longest ISIs is here defined as the top 5% of the ISI distribution (if only 80 spikes or fewer were recorded, we instead took the four longest ISIs; for fewer than 11 spikes, no BI was computed), and the BI is then given as

$$BI = \frac{total\ time\ of\ longest\ ISIs}{total\ sample\ time} \times \frac{mean\ duration\ of\ the\ longest\ ISIs}{\frac{total\ sample\ time}{total\ number\ of\ ISIs}} \quad (2)$$

Larger values of the BI indicate a stronger tendency of burst firing.

Statistical Testing

The effects of ivabradine on the measured response parameters were statistically evaluated at the population level with a Wilcoxon rank-sum test. For the analyses of the responses to repeated white noise presentation, this was used to compare the differences between the first and subsequent white noise presentations of each cell in the ivabradine group with those in the sham group.

The effect of ivabradine on spontaneous activity was evaluated by computing a normalized difference in firing rate and by computing the ratio of the burst index before and after drug administration. These distributions were statistically tested for differences of the median from zero and unity, respectively, with a sign test. The use of the relatively

Investigative Ophthalmology & Visual Science

conservative sign test here takes into account that positive and negative changes of the ratio of burst indices are of different scales. Significance was assessed at the 5% level. Error bars show SEMs. To summarize the distribution of extracted parameters across populations of cells, we used box plots, which display the median and the range from the first to the third quartile (interquartile range [IQR]) by a line and a box, respectively, with whiskers extending to the most extreme values within 1.5 × IQR and outliers beyond 1.5 × IQR marked by separate data points.

Results

Pharmacologic HCN Channel Block Delays Ganglion Cell Responses

To analyze how pharmacologic block of HCN channels in the retina by ivabradine affects responses of ganglion cells under visual stimulation, we recorded spiking activity from ganglion cells in isolated mouse retinas with multielectrode arrays and assessed the cells' temporal filtering characteristics in response to white noise stimulation. For this analysis, the retina was illuminated with spatially homogeneous light whose intensity was randomly chosen from a Gaussian distribution at a rate of 30 Hz. The temporal filtering characteristics of the recorded ganglion cells were then assessed by correlating the measured spike times with the applied stimulus, that is, by computing the spike-triggered average,[30] which corresponds to the average stimulus sequence that preceded a spike (Fig. 1A). The spike-triggered average can be viewed as the temporal stimulus filter of the cell.

To compare filter characteristics with and without drug administration, we applied the white noise stimulus once before drug administration and then repeatedly in the presence of the drug and after washout. Focusing first on the comparison of On and Off ganglion cells, we found that ivabradine strongly altered the shapes of temporal filters by broadening and delaying the filters for both classes of cells (Fig. 1B, left column). Some of these changes reversed after washout of the drug, yet reversal was not complete. This is not surprising, because the applied HCN channel blockers are notoriously difficult to wash out.[20,35] Thus, as a control, we performed sham experiments where the same experimental sequence was applied, including a switch between different sources of the perfusion solution at the time when normally application of ivabradine would start, but with the drug absent from the perfusion. These sham experiments showed that the filter shapes were stable over the course of the recording (Fig. 1B, right column), indicating that the observed changes in filter shape under drug administration were indeed a consequence of the drug and not simply a run-down effect over the course of the experiment.

To assess the filter changes on a population level, we first extracted the time to peak of the filters as a measure of the response delay. We found that the average time to peak of the filters significantly increased by approximately 30 to 40 ms for both On and Off cells under ivabradine (Fig. 1D). The control group, on the other hand, had a much smaller change in time to peak of up to 10 ms, presumably owing to mild adaptation effects over the course of the experiment, indicating that the increased response delay is indeed an effect of the drug application. Note that the changes in the filters did not occur immediately after drug administration, but developed slowly over time, becoming significant only for the second presentation of the white noise stimulus after the beginning of drug administration. This is in line with previous reports regarding a delayed effect of HCN channel blockers.[20,35,36]

The temporal filters of the ganglion cells typically have a biphasic shape: the initial peak, which is positive for On cells and negative for Off cells, is followed by a secondary peak of opposite sign, which may result from inhibitory input that follows the initial excitation or from negative feedback, such as adaptation or synaptic depression.[33,37,38] Thus, to test whether ivabradine also had specific effects on the filter shape, we analyzed the biphasic structure of the filter by computing a biphasic index that measures the relative size of the secondary peak compared with the primary peak (see Methods). We found that filter biphasicness was also affected by ivabradine, yet, in contrast to the changes in response delay, the changes in biphasicness had opposite signs for On cells compared with Off cells, with increased biphasicness for On cells and decreased biphasicness for Off cells (Fig. 1E). Thus, the drug-induced changes of ganglion cell temporal filters go beyond a simple slowing down of response kinetics.

Reduced Sensitivity to High Temporal Frequencies Under HCN Channel Block

Previous studies of the effect of HCN channel block on retinal photoreceptors and bipolar cells had shown pronounced shifts from band-pass to low-pass filtering.[20,22,39] To check whether the observed changes of the ganglion cell filters in the time domain also correspond to such a shift toward low-pass filtering, we calculated power spectra of temporal filtering (see Methods). As illustrated by the power spectra of the two sample cells (Fig. 1C) and corroborated by the population analysis (Fig. 1F), we found that this was indeed the case. After drug administration, power spectra showed relatively increased power for frequencies below about 2 Hz and a corresponding power decrease for higher frequencies, as quantified on the population level for the frequency band from 3 to 10 Hz. Control experiments, on the other hand, showed relatively constant power spectra, indicating that the observed changes of power spectra were indeed a consequence of HCN channel block.

Increase of Response Latencies to Light Intensity Steps Under HCN Channel Block

As an alternative assessment of the temporal dynamics of light responses, we measured latencies of the spiking responses under stimulation with steps in light intensity (Fig. 2). We found that latencies increased considerably for both On and Off cells under ivabradine (average latency increase 11.5 ± 1.4 ms [mean ± SEM] for On cells and 31.8 ± 5.8 ms for Off cells), in line with the delay of the filters observed under white noise stimulation (Fig. 1). These changes were significantly stronger than observed under control conditions ($P = 0.003$ for On cells and $P = 0.007$ for Off cells), which displayed only small latency increases over time (4.2 ± 1.0 and 0.2 ± 4.3 ms for On and Off cells, respectively).

Differential Effects of HCN Channel Block on Sensitivity of On and Off Cells

The filters analyzed in the previous section denote which temporal features best activate the ganglion cells. To analyze how this activation is translated into the neuronal response, we constructed a full linear-nonlinear (LN) model[30] for each cell by computing the nonlinearity that relates the output of the stimulus filter to the elicited firing rate (Fig. 3). To analyze changes in the nonlinearity, we used a parametric fit to extract the maximal firing rate as the rate where the response saturated, the gain as the maximal slope of the nonlinearity, and the setpoint as an approximation of the threshold (see Methods).

Investigative Ophthalmology & Visual Science

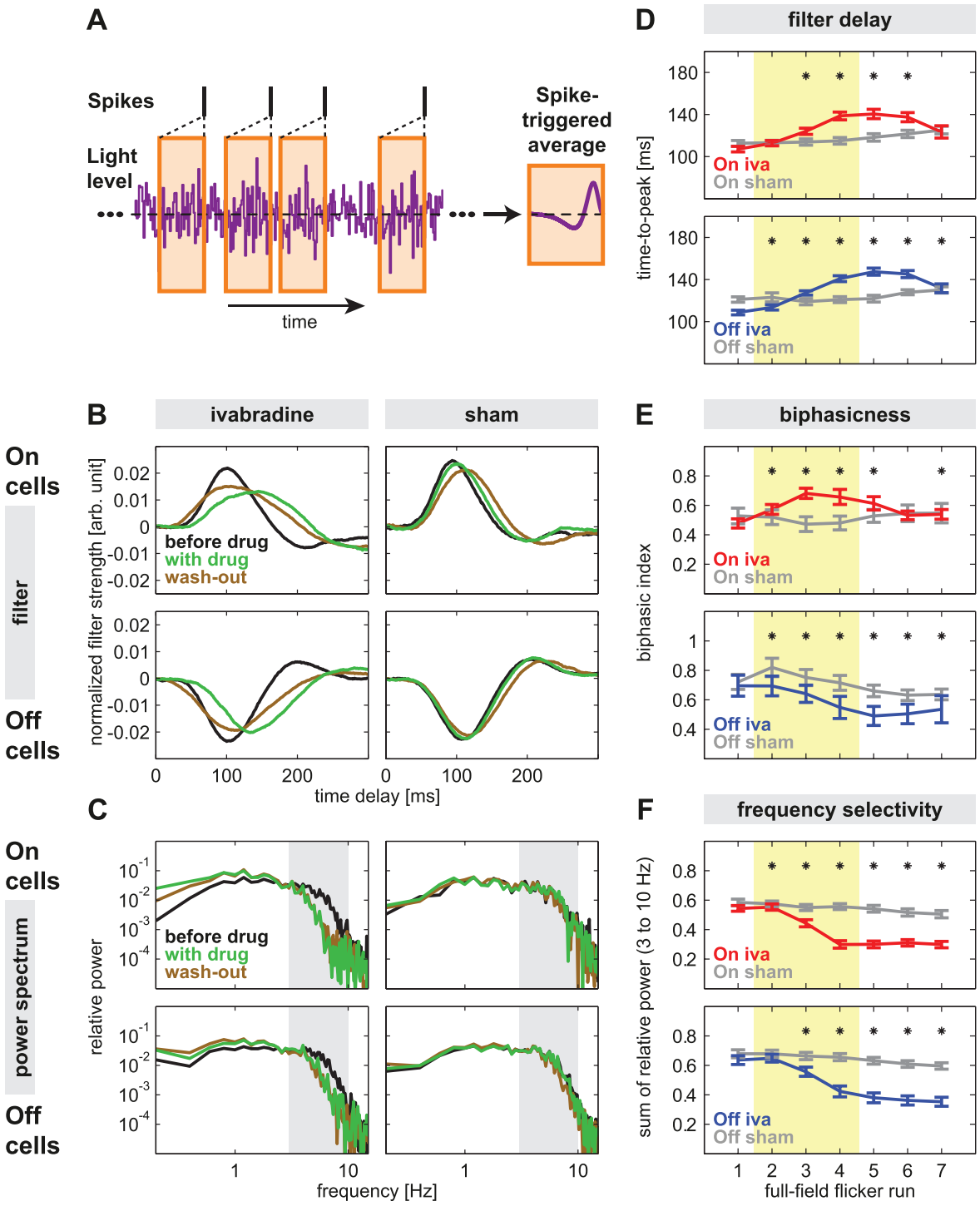

Figure 1. Effect of ivabradine on temporal filtering. (**A**) Schematic depiction of the reverse-correlation analysis. Spikes are measured in response to a pseudo-random sequence of light intensity, fluctuating around a mean background level. For each spike, the preceding stimulus sequence is collected, and the average of all these sequences (spike-triggered average) yields the cell's temporal stimulus filter. (**B**) Filters obtained by the first (*black*, before drug), fourth (*green*, with drug), and last run (*brown*, after washout) of white noise stimulation for representative On and Off cells. (**C**) Power spectra of the filters shown in **B**. The gray regions mark the analyzed band of 3 to 10 Hz. (**D**) Population analyses of time to peak over all seven stimulus repeats, separately for On cells (*red*, $N = 58$ in ivabradine group and $N = 36$ in sham group) and Off cells (*blue*, $N = 34$ in ivabradine group and $N = 39$ in sham group), each compared with corresponding cells of the sham group (*gray*). (**E**) Population analysis of the biphasicness of the filters. Biphasicness was computed as the size of the secondary filter peak relative to the primary peak. (**F**) Population analysis of relative power of temporal filters between 3 and 10 Hz. *Asterisks* in **D**–**F** denote significant differences between drug and sham groups after normalizing values to the first run. The full-field flicker run number in **D**–**F** refers to the repeated presentation of identical white noise sequences, each 6 minutes long and separated by approximately 2 minutes of recovery in the dark; the *shaded region* marks the period of drug delivery.

Investigative Ophthalmology & Visual Science

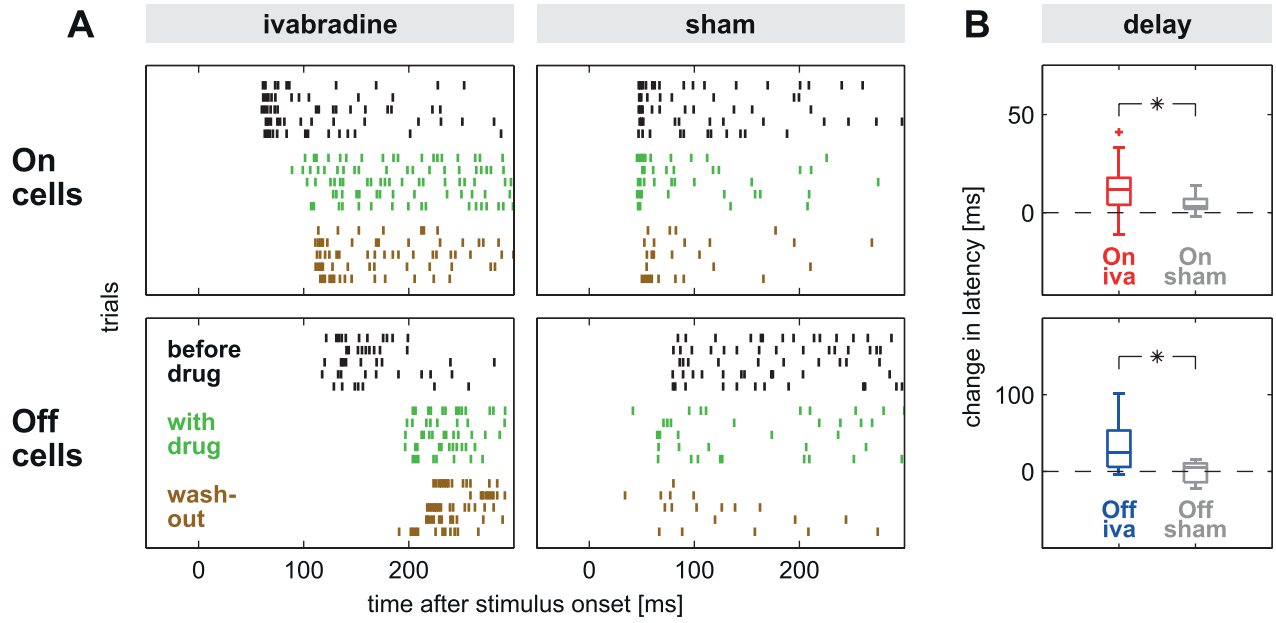

Figure 2. Effect of ivabradine on response latency. (**A**) Examples of spike trains following onset (*top*) and offset (*bottom*) of bright illumination before (*black*), during (*green*), and after (*brown*) drug application. *Right*: Examples from sham group. (**B**) Box plots displaying the distributions of the change in response latency for different populations, analyzing responses after light onset for On cells ($N = 59$ in ivabradine group and $N = 18$ in sham group) and responses after light offset for Off cells ($N = 29$ in ivabradine group and $N = 11$ in sham group). *Asterisks* denote significant differences between drug and sham groups.

We found that nonlinearities of On and Off cells were affected in different ways by ivabradine. On cells often showed a considerable reduction in gain, whereas Off cells had relatively stable gain values or even showed a slight increase of gain when HCN channels were blocked (Fig. 3B). For the setpoint, on the other hand, we found that On cells displayed no significant change compared to control, whereas Off cells showed a substantial increase of the setpoint under HCN channel block (Fig. 3C), corresponding to an increased activity threshold. As a consequence, the baseline firing rate, that is,

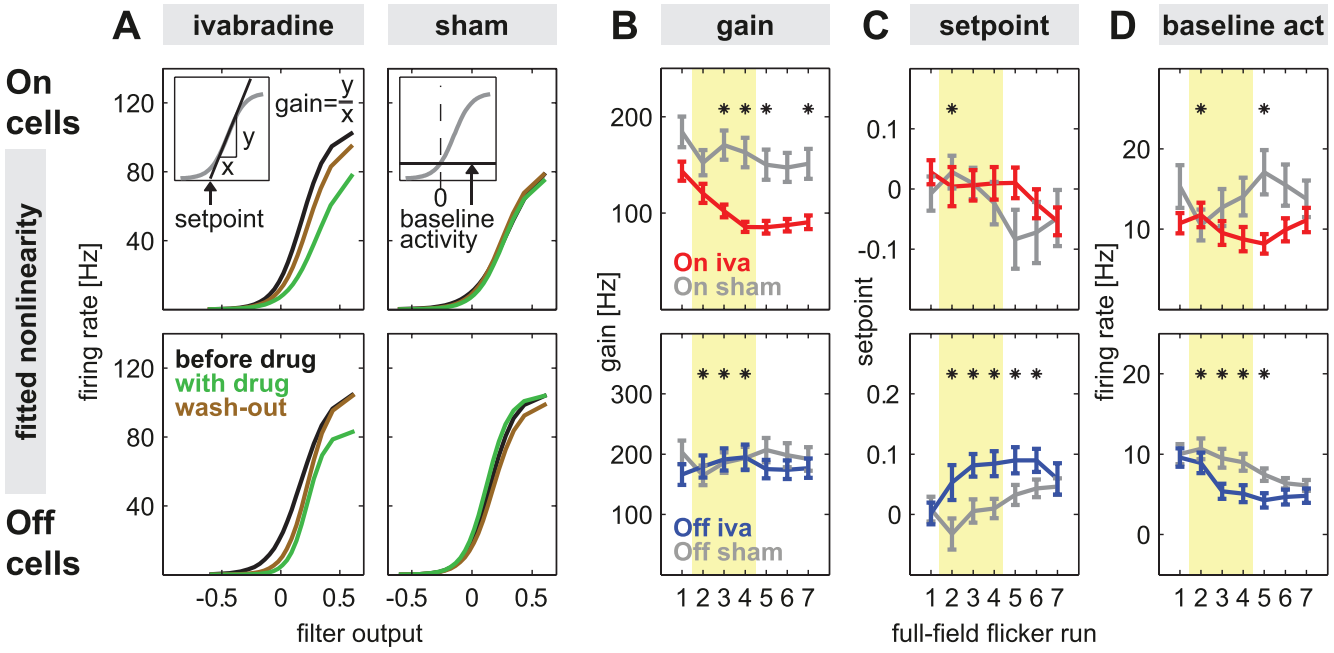

Figure 3. Effect of ivabradine on sensitivity and baseline activity. (**A**) Examples of fitted nonlinearities obtained by the first (*black*, before drug), fourth (*green*, with drug), and last (*brown*, after washout) run of white noise stimulation. *Insets* illustrate the calculation of parameters that were used to quantify changes of nonlinearities. (**B–D**) Population analysis of gain (**B**), setpoint (**C**), and baseline activity (**D**) over all seven runs for the same groups of cells as analyzed in Figure 1. *Asterisks* denote significant differences between drug and sham groups after normalizing values to the first run. As in Figure 1, the full-field flicker run number in **B–D** refers to the repeated presentation of identical 6-minute white noise sequences, separated by approximately 2-minute recovery periods; the *shaded region* marks the period of drug delivery.

Investigative Ophthalmology & Visual Science

the firing rate for zero filter output, strongly decreased for Off cells under ivabradine, but not for On cells (Fig. 3D). The maximal firing rate was not significantly affected by ivabradine in either On or Off cells (data not shown). Together, this means that nonlinearities of On and Off cells were differentially affected by HCN channel block. For On cells, nonlinearities became less steep, whereas for Off cells, nonlinearities rather shifted rightward toward a higher threshold and decreased baseline activity.

Spontaneous Firing Increased for On Cells, but Decreased for Off Cells Under HCN Channel Block

The differential effects of HCN channel block on the baseline firing rate of On and Off ganglion cells under white noise stimulation led us to hypothesize that spontaneous spiking activity could also be differentially affected among these cells. We therefore measured spontaneous activity over extended periods before and during application of ivabradine (Fig. 4A). As the background light intensity can have an influence on spontaneous activity,[40] the measurements were performed under homogeneous static illumination in the mesopic range at the level of the mean luminance of the temporal white noise experiments to allow direct comparison. To test the generality of our findings, we also performed measurements of spontaneous activity under brighter illumination in the photopic range.

As illustrated by sample On and Off ganglion cells in Figure 4A, we observed that HCN channel block led to a slow, persistent change in spontaneous activity after the onset of drug adminstration under mesopic as well as under photopic light conditions. Over the course of several minutes, spontaneous activity increased in the On ganglion cell and decreased in the Off cell. To quantify this observation over the population of all recorded ganglion cells, we compared the rates of spontaneous firing in consecutive windows of 200 seconds duration.

Figure 4B shows how the spontaneous activity had changed after 20 minutes of drug administration. For On cells, ivabradine led to a systematic increase in spontaneous activity at both light levels, whereas Off cells rather displayed a decrease in activity. These systematic changes were not observed under control conditions without the drug, except for some decrease in spontaneous activity for Off cells under photopic conditions, which may reflect a slow adaptation effect.[40]

The changes in spontaneous activity built up slowly over time. This is analyzed in Figure 4C, where the change in spontaneous activity, compared with the level prior to drug administion, is displayed in consecutive windows of 200 seconds after the onset of drug application. For example, the decrease in spontaneous activity in Off cells under mesopic conditions became significant only after 1000 seconds, and in all cases, the changes of spontaneous activity under ivabradine administration became more pronounced over time. At the end of the 20-minute recording, during the last of the six 200-second windows, the activity increase for On cells, as well as the activity decrease for Off cells under both mesopic and photopic conditions, were significant (sign test, $P < 0.02$ in all cases). These changes in spontaneous activity furthermore differed significantly from any changes observed under control conditions (ranksum test, $P < 0.001$ in all cases), except for Off cells under photopic conditions, owing to a comparable decrease of spontaneous activity in the sham group.

Increased Bursting by Off Ganglion Cells During HCN Channel Block

Besides the changes in firing rate, the comparison of spontaneous activity before and during ivabradine administration also revealed alterations in the occurrence of spike bursts. Figure 5A shows an example of an Off ganglion cell with fairly regular firing before drug administration and pronounced bursting in the presence of ivabradine. The transition from regularly firing to bursting is also reflected in the return map of ISIs (Fig. 5B), which displays the relation of consecutive ISIs. The clustered structure of the return map during drug administration indicates that distinctly long (interburst) intervals were generally preceded and followed by short (inner-burst) intervals, whereas no such clear structure is apparent before drug administration.

We quantified the occurrence of bursting by computing a burst index (BI) (see Methods), which assesses how much time the neuron spent in its longest ISIs and how long these intervals were compared with the average ISI.[34] The analysis showed that the activity of Off ganglion cells generally became more burst-like under ivabradine administration, in particular under photopic conditions (Fig. 5C). On ganglion cells, on the other hand, displayed a mild, yet significant reduction of the BI under mesopic illumination conditions. To check whether these differential effects in bursting activity persisted under temporally structured visual stimulation, we also calculated the BI for the response to white noise stimulation before and during ivabradine application. Here, we found a similar picture (Fig. 5D) with strongly increased bursting by Off cells and small or no effects for On cells. Thus, the organization of the spontaneous spiking activity into bursts was differentially affected by ivabradine administration in On and Off ganglion cells in both spontaneous activity and stimulus-evoked activity.

Effects of HCN Channel Block on On-Off Cells

Thus far, we have focused on comparing On cells and Off cells in how they are affected by the HCN channel block. However, in addition to these major classes of ganglion cells, the retina also contains On-Off ganglion cells, which respond to both increases and decreases in light intensity. To investigate how On-Off cells are affected by the HCN channel block, we identified these cells according to their responses under steps in light intensity (see Methods) and then analyzed the drug-induced changes in filter shapes (Fig. 6A), changes in spontaneous activity (Fig. 6B), and changes in bursting structure (Fig. 6C). We did not analyze sensitivity changes via the nonlinearity of the full LN model because On-Off cells are not well described by a single nonlinear transformation, and obtained nonlinearities are often nonmonotonic.[41,42]

We found that temporal filtering in On-Off cells showed a similar increase in response delay and shift to low-pass filtering as had been observed for both On and Off cells. Filter biphasicness changed only mildly, with the small decrease in biphasicness becoming significant compared with control data only after application of ivabradine was stopped. Spontaneous activity and bursting were not significantly affected by ivabradine application. Thus, drug-induced changes that were consistent between On and Off cells, such as the changes in filter delay and low-pass filtering, were also displayed similarly by On-Off cells. For those phenomena where changes in On cells and Off cells went in opposite directions, on the other hand, On-Off cells displayed hardly any change, suggesting that these differential effects on the On and Off pathways may cancel when they converge onto On-Off cells.

Cell-by-Cell Relation of Changes in Spontaneous and Evoked Activity

The HCN channel block affected both the baseline firing rate under visual stimulation and the spontaneous activity

Investigative Ophthalmology & Visual Science

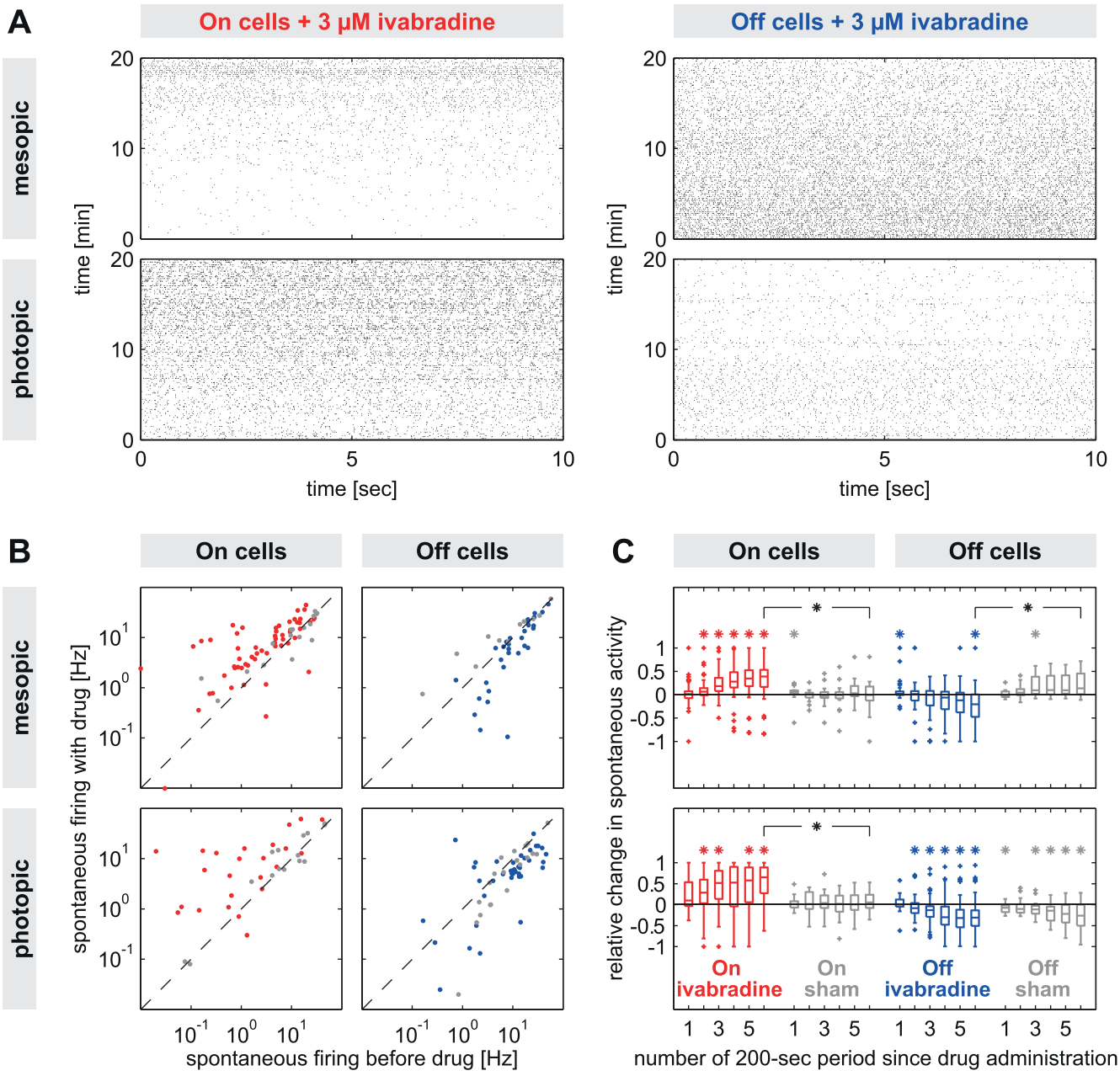

Figure 4. Effect of ivabradine on spontaneous activity. (**A**) Examples of 20-minute recording of spontaneous activity, separated into consecutive stretches of 10 seconds each, for two On cells (*left*) and two Off cells (*right*), following the onset of ivabradine administration under mesopic (*top*) and photopic (*bottom*) light conditions. (**B**) Comparison of firing rates during 200-second windows before drug administration (*x*-axis) and after 20 minutes in the presence of the drug (*y*-axis), separately for On cells (*left, red*; mesopic: $N = 60/18$ for ivabradine/sham; photopic: $N = 26/15$ for ivabradine/sham) and Off cells (*right, blue*; mesopic: $N = 33/11$ for ivabradine/sham; photopic: $N = 42/20$ for ivabradine/sham). Each data point corresponds to a ganglion cell; gray data points denote cells from sham group. (**C**) Box plots of change in spontaneous firing, relative to the 200-second period before drug application. Same data as in **B**. *Asterisks* denote significant changes within each group and significant differences between the changes in the drug and sham group for the final 200-second period.

under constant illumination. Similarly, we observed changes in bursting activity both in the spontaneous and in the visually evoked activity. We therefore asked whether the changes in firing rate and the changes in bursting activity were related on a cell-by-cell basis between spontaneous and visually evoked activity. When we compared the changes in spontaneous firing rate and the changes in baseline activity under mesopic conditions (Fig. 7A), we found a strong correlation ($r = 0.61$, $P < 10^{-4}$), confirming that spontaneous activity in the absence of a temporally structured stimulus and baseline activity during continuous stimulation with white noise were affected similarly by the administration of the HCN channel block. Note that the changes in baseline activity under stimulation were here computed from white noise stimulation once before and once after the measurement of spontaneous activity and therefore present a different set of recordings than the ones analyzed for Figure 3D, where seven consecutive runs of white noise stimulation had been applied. Note further that Figure 3D showed essentially no change in baseline activity for On cells, whereas Figure 7A indicates an increase in baseline activity for On cells; this is a discrepancy that we

Investigative Ophthalmology & Visual Science

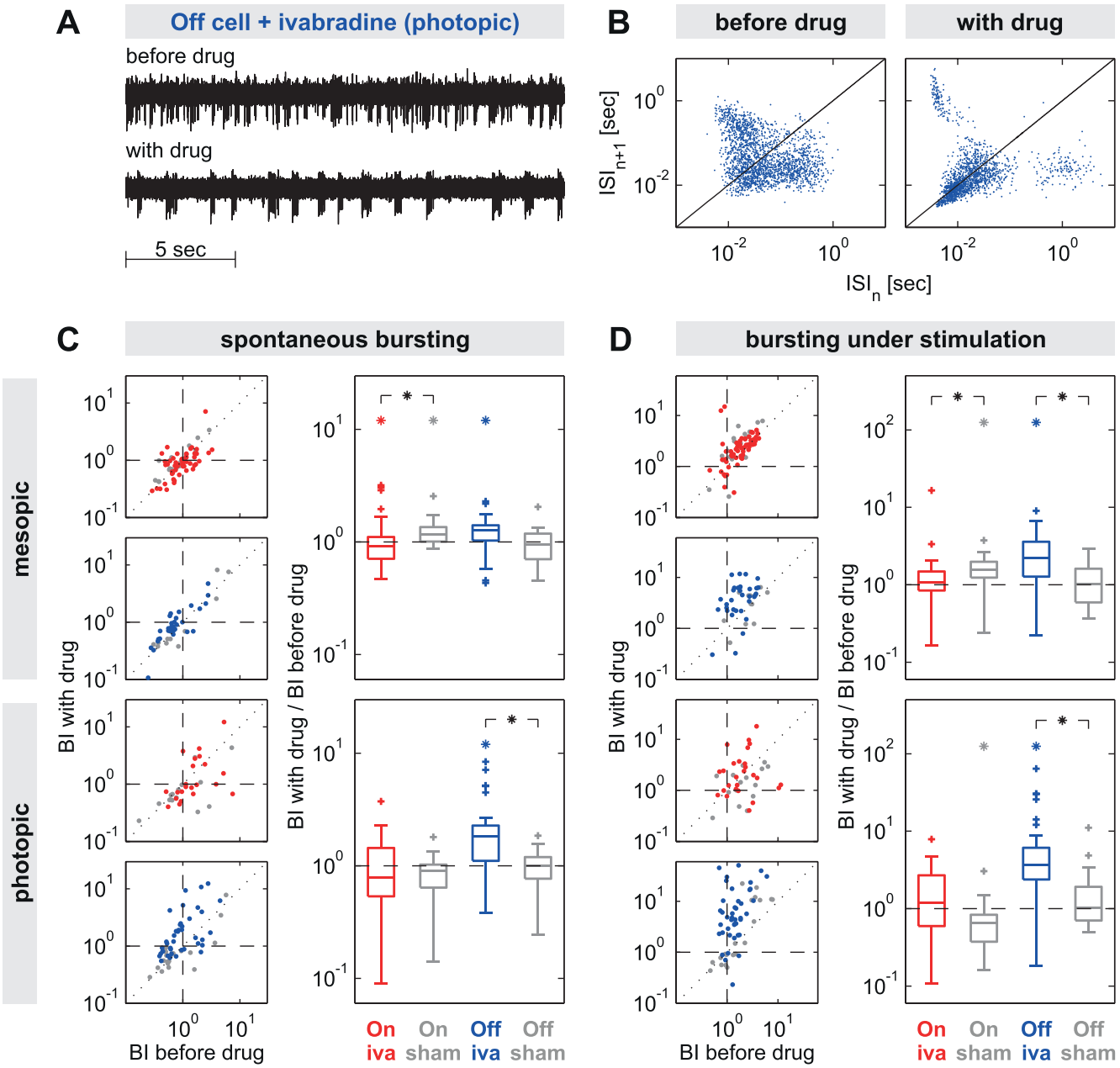

Figure 5. Effect of ivabradine on burst firing. **(A)** Sample voltage traces of spontaneous activity, recorded from an Off cell before drug administration (*top*) and after 20 minutes of ivabradine administration (*bottom*). **(B)** Return maps of ISIs for the sample neuron of **A**, showing the dependence of ISIs on the preceding ISI. Data come from the last 200 seconds of spontaneous activity before drug application (*left*) and from the last 200 seconds of the 20-minute recording in the presence of the drug (*right*). **(C)** BIs for spontaneous activity under mesopic light levels (*top*) and photopic light levels (*bottom*). Scatter plots on the *left* compare BIs during the last 200 seconds before drug administration and during 200 seconds after 20 minutes of drug administration separately for On cells (*red*; mesopic: $N = 54/17$ for ivabradine/sham; photopic: $N = 22/15$ for ivabradine/sham) and Off cells (*blue*; mesopic: $N = 31/11$ for ivabradine/sham; photopic: $N = 40/19$ for ivabradine/sham). *Gray data points* correspond to cells from the sham group. Box plots on the *right* display the relative changes of BIs. *Asterisks* denote significant changes within each group and significant differences between the changes in the drug and sham group. **(D)** Same as **C**, but for BIs computed from activity under white noise stimulation for On cells (*red*; mesopic: $N = 60/18$ for ivabradine/sham; photopic: $N = 26/15$ for ivabradine/sham) and Off cells (*blue*; mesopic: $N = 33/11$ for ivabradine/sham; photopic: $N = 42/20$ for ivabradine/sham).

attribute to experimental variability, as the determination of nonlinearities is relatively sensitive to noise.

When we compared the change in bursting during spontaneous and evoked activity on a cell-by-cell basis, we also found a strong correlation ($r = 0.39$, $P < 10^{-4}$), which was even more pronounced when we only considered Off cells ($r = 0.49$, $P < 10^{-4}$), which were the cells for which changes in bursting were strongest. Thus, the drug-induced changes in firing rate and bursting activity were strongly related on a cell-by-cell basis between spontaneous and stimulus-evoked activity.

Discussion

We investigated how pharmacologic HCN channel block affects the spontaneous and stimulus-evoked activity of retinal

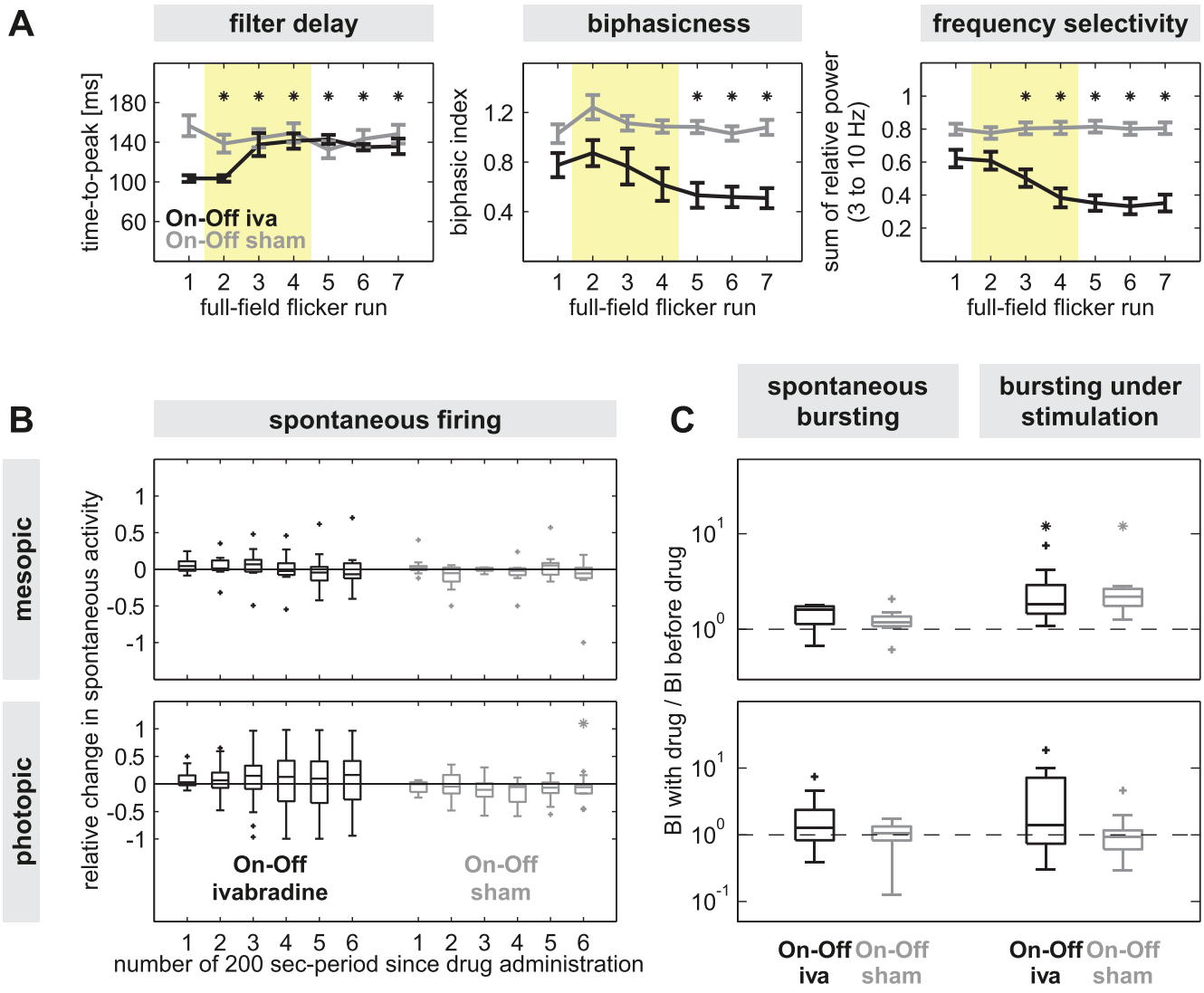

Figure 6. Analysis of On-Off ganglion cells. (**A**) Drug-induced changes in temporal filtering, as measured by the filter delay (*left*), biphasicness (*center*), and frequency selectivity (*right*), analogous to Figures 1D–1F. $N = 18/26$ for ivabradine/sham. *Asterisks* denote significant differences between drug and sham groups after normalizing values to the first run. As in Figure 1, the full-field flicker run number refers to the repeated presentation of identical 6-minute white noise sequences, separated by approximately 2-minute recovery periods; the *shaded region* marks the period of drug delivery. (**B**) Drug-induced changes in spontaneous firing rates, analogous to Figure 4C. $N = 11/9$ for ivabradine/sham under mesopic illumination and $N = 25/14$ under photopic illumination. (**C**) Changes in bursting activity, analogous to the box plots in Figures 5C and 5D. $N = 11/9$ for ivabradine/sham for mesopic illumination and $N = 25/14$ for photopic illumination, with one cell from the sham group excluded in the analysis of mesopic spontaneous bursting for lack of sufficient spiking. *Asterisks* denote significant changes.

ganglion cells, the output neurons of the retina. The two main lines of results are (1) the altered temporal kinetics of stimulus encoding, expressed by a change in filter delay and a shift toward low-pass filtering by the ganglion cells, which occurred in a similar fashion for On and Off ganglion cells; and (2) the changes in filter biphasicness, sensitivity, baseline activity, and spontaneous activity, which showed opposite effects in On and Off cells.

Relation to Previous Work

Previous work on the effect of HCN channel block on neuronal activity in the retina had focused on responses of photoreceptors and bipolar cells. These studies had revealed delayed responses and a reduced processing of high-frequency stimuli by photoreceptors[20,22] and bipolar cells[39] under pharmacologic HCN channel block. This is consistent with our observed changes in ganglion cell response kinetics, indicating that these effects originate in photoreceptors and are faithfully transmitted through the retinal network. Indeed, ganglion cells in HCN1 knockout mice displayed similar shifts toward low-pass filtering.[24] Furthermore, measurements of electroretinograms after genetic or pharmacologic HCN channel block confirmed the reduced encoding of flicker or sinusoidal light stimulation in vivo.[5,21,23] Mechanistically, the reduced encoding of higher temporal frequencies under mesopic conditions is thought to result from saturation in the retinal network induced by prolonged activation of rod photoreceptors.[24]

However, another observation in photoreceptors was the increased response amplitude under light stimulation,[22] which suggests a higher gain under the HCN channel block. By contrast, we here found that, for ganglion cells, sensitivity under ivabradine rather decreases, as expressed by reduced gain for On cells and increased threshold for Off cells. Also, the

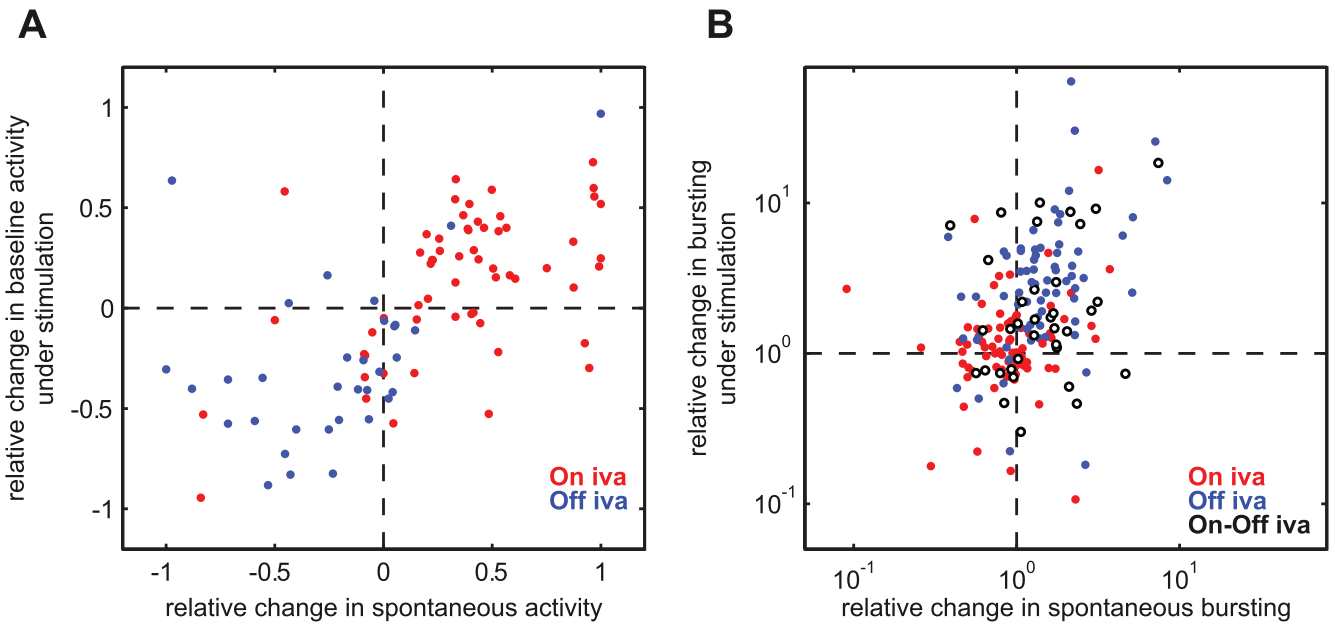

Figure 7. Cell-by-cell comparison of drug-induced changes in firing rate and bursting between spontaneous and visually evoked activity. (**A**) Baseline activity during white noise stimulation versus spontaneous activity on a cell-by-cell basis (*red*: On cells, $N = 60$; *blue*: Off cells, $N = 33$; On-Off cells were not analyzed because no nonlinearities were obtained to assess baseline activity under stimulation). The relative change in baseline activity under stimulation was computed as the difference of baseline activity with and without drug, normalized by the sum of both. The relative change in spontaneous activity similarly corresponds to the normalized differences with and without drug, using the 200-second period before drug administration and the last 200-second period at the end of the 20-minute recording in the presence of the drug. (**B**) Bursting activity during white noise stimulation versus bursting in spontaneous activity (*red*: On cells, $N = 76$; *blue*: Off cells, $N = 71$; *black*: On-Off cells, $N = 36$). The relative changes were computed as the ratios of burst indices with and without drug administration.

effects of ivabradine on filter biphasicness, spontaneous activity, and bursting by ganglion cells, in particular the fact that On and Off ganglion cells display opposing changes, do not directly follow from the previous findings of altered kinetics in photoreceptors and bipolar cells. Thus, new mechanistic hypotheses are required to explain the differential effects of the HCN channel block on On and Off ganglion cells.

Mechanistic Interpretation

When considering how the strong effects of the HCN channel block on photoreceptor responses may influence the ganglion cell responses, one has to keep in mind that the synaptic transmission and network processing in the retinal network may further shape the effects on neuronal activity. In particular, signal transmission is often nonlinear[43–45] and influenced by negative feedback, such as adaptation and synaptic depression.[46,47] We here hypothesize that the differential effects of the HCN channel block on On and Off ganglion cells result from interactions between the drug-induced changes in photoreceptor activation and the signal transmission at the synapse between photoreceptors and bipolar cells. Under control conditions, the current through the HCN channels counteracts hyperpolarization of the photoreceptor.[12,13] Blocking the channels therefore leads to prolonged hyperpolarization events, which under continuous light exposure is expected to result in a hyperpolarized baseline potential. This can, in fact, be observed in membrane potential recordings of photoreceptors.[22] The sustained hyperpolarization results in a reduction of baseline neurotransmitter release, which, in turn, leads to sustained activation of On bipolar cells via the sign-inverting function of the cells' metabotropic glutamate receptors and a reduced baseline membrane potential in Off bipolar cells via their sign-conserving ionotropic glutamate receptors.

Thus, On bipolar cells will show increased baseline activation under ivabradine. As a result, the gain in the On pathway will likely decrease, for example, because of synaptic depression at the bipolar-to-ganglion cell synapse.[48,49] This is consistent with our observation that the gain of the cells' nonlinearities was reduced under ivabradine (Fig. 3B). Increased activation of such negative feedback mechanisms would also explain the increased biphasicness observed in the filters of On ganglion cells (Fig. 1E) because the secondary filter peak typically reflects such feedback mechanisms.[33,37,38] For the Off pathway, on the other hand, the decreased baseline membrane potential of Off bipolar cells means that stronger stimuli are required to eventually reach threshold for triggering spikes in Off ganglion cells, consistent with the increased threshold of Off cell nonlinearities (Fig. 3C). One important ingredient here is likely the nonlinear, threshold-like signal transmission between bipolar and ganglion cells[50–53] so that transient events of bipolar cell activation are more likely to be filtered out at this stage when the baseline activation is reduced. Furthermore, the resulting reduction in activity through reduced excitatory drive also means that negative feedback mechanisms, such as synaptic depression, will be less strongly activated, explaining the decrease in filter biphasicness (Fig. 1E).

Thus, the sustained photoreceptor hyperpolarization under ivabradine can explain both the drug-induced decrease in gain for the On pathway (Fig. 3B) and the higher threshold for the Off pathway (Fig. 3C), as well as the differential changes in filter biphasicness (Fig. 1E). Moreover, the same mechanism also provides an explanation for the differential changes in spontaneous activity (Fig. 4) because the increased baseline activation of On bipolar cells will result in increased spontaneous firing rates of On ganglion cells, whereas the decreased baseline activation of Off bipolar cells causes a decrease in spontaneous activity for Off ganglion cells. Finally, the latter may also underlie

the increased bursting activity observed for Off ganglion cells (Fig. 5) because the prolonged periods of subthreshold activity in the Off pathway leads to transiently increased sensitivity both in the synaptic transmission from bipolar to ganglion cells and in the spike generation process of the ganglion cell. Thus, spikes may come in bursts once activation either from noise or from visual stimulation is strong enough to pass the nonlinear bipolar-to-ganglion cell signal transmission and reach spiking threshold in the ganglion cells. Indeed, it has been observed that spiking activity for Off ganglion cells can become much more burst-like upon hyperpolarization.[54]

Differential Effects of Ivabradine in On and Off Pathways as a Potential Cause of Phosphene Perception

Luminous phenomena, so-called phosphenes, are the most frequent side effects in patients treated with ivabradine. This drug is a specific bradycardic agent, which reduces the heart rate by blocking the pacemaker current I_f in the sino-atrial node of the heart.[55] In contrast to other chronotropic (i.e., affecting the heart rate) drugs like β-blockers, ivabradine specifically lowers the heart rate without negative inotropic (i.e., affecting strength of the heart muscle) effects.[56,57] Sole reduction of the heart rate diminishes cardiac work and oxygen consumption and improves oxygen supply of the heart muscle by increasing coronary perfusion in consequence of a prolonged diastole.[58,59] Therefore, ivabradine is considered a promising approach to reduce angina pectoris symptoms and improve cardiovascular outcome of patients with stable coronary artery disease.[15,25,60] Approximately 15% of patients treated with ivabradine report the perception of phosphenes.[25]

The induction of phosphenes by ivabradine is thought to follow from the block of HCN channels in the retina.[25,26] In particular, the reduced band-pass filtering of the retina has been thought to be critical.[19] The proposed mechanism suggests that noise events in rod photoreceptors, caused by thermally induced spontaneous isomerization of the photopigment, are enhanced in amplitude when the high-pass-filtering effect of HCN channels is abolished. Thus, photoreceptor noise that is normally filtered out by the nonlinear synaptic transmission between rods and bipolar cells[61,62] will then be able to overcome the transmission threshold and cause downstream retinal activity. It seems likely that this mechanism is most effective at low light intensities, when vision is dominated by rod signals and photoreceptor noise contributes a sizeable component to the overall photoreceptor activity.

However, phosphenes under ivabradine administration occur also during light exposure.[19] Furthermore, they may be connected to visual stimulation, as they have been reported to be associated with abrupt changes in light intensity[25] and are enhanced by watching television,[26] which is likely dominated by cone-mediated vision in the photopic regime. Under such viewing conditions, noise from spontaneous isomerizations is swamped by visually evoked activity in the photoreceptors, and there is no effective thresholding of noise at the transmission to bipolar cells. Thus, additional mechanisms appear necessary to explain phosphenes during visual activity. Our observations of differential changes in On and Off ganglion cells point to such a mechanistic explanation for moderate to high light intensities. We hypothesize that the relative increases of baseline activity and spontaneous firing in On ganglion cells and the prolonged activity gaps between spike bursts in Off cells under ivabradine lead to an imbalance of On and Off signals that emerge from the retina. This imbalance could be interpreted by downstream brain areas as episodes of local, transient brightening. We suggest that, mechanistically, this imbalance stems from a light-evoked sustained hyperpolarization of photoreceptors under the HCN channel block, resulting in opposing shifts of baseline activation for On and Off bipolar cells. This is followed by signal thresholding and gain control at the bipolar-to-ganglion cell synapse, leading to the structuring of Off cell responses into prolonged periods of silence and intermittent bursting. This mechanism for phosphene generation under visual stimulation is complementary to the hypothesis based on spontaneous isomerizations in darkness.

Given that phosphenes may thus be caused by fairly basic changes in the response structure, it is interesting to ask whether there are other ways of evoking such changes, for example, through basic features of visual stimulation. One hypothesis may be that response properties could be affected in similar fashion when background illumination changes. However, going to a different light level can evoke much more substantial alterations in response properties, including fundamental changes in the responses used to classify cells as On, Off, or On-Off,[63] and how perception remains stable despite these alterations is not yet understood. Alternatively, one may consider very slow, continuous increases in mean light intensity, aimed at providing sustained activation of the On pathway. Exploring the effects of such variations in stimulus context may provide interesting directions for future research.

The relationship of changed spontaneous activity and false sensory perception has also been reported for other sensory systems, for example, relating to tinnitus[64,65] or neuropathic pain.[66,67] The increased spontaneous activity in auditory centers leading to sound perception in tinnitus may be seen as a direct analogy to the increased activity in On-type retinal cells as a cause for phosphene perception. These connections between altered processing in early sensory systems and perceptual phenomena without a corresponding stimulus provide an opportunity for insight into how neural signaling underlies sensory perception, and a better understanding of the underlying causality may aid therapeutic interventions for counteracting undesired perceptual phenomena.

Acknowledgments

The authors thank Stylianos Michalakis for discussions that helped initiate this project.

Supported by an independent research grant from Novartis Pharma GmbH, Nuremberg, the Deutsche Forschungsgemeinschaft through the Collaborative Research Center 889 "Cellular Mechanisms of Sensory Processing," project C1, and the European Research Council (ERC) under the European Union's Horizon 2020 research and innovation programme (Grant 724822).

Disclosure: **S. Bemme**, None; **M. Weick**, None; **T. Gollisch**, None

References

1. Biel M, Wahl-Schott C, Michalakis S, Zong X. Hyperpolarization-activated cation channels: from genes to function. *Physiol Rev*. 2009;89:847–885.
2. Wahl-Schott C, Biel M. HCN channels: structure, cellular regulation and physiological function. *Cell Mol Life Sci*. 2009; 66:470–494.
3. Müller F, Scholten A, Ivanova E, Haverkamp S, Kremmer E, Kaupp UB. HCN channels are expressed differentially in retinal bipolar cells and concentrated at synaptic terminals. *Eur J Neurosci*. 2003;17:2084–2096.
4. Stradleigh TW, Ogata G, Partida GJ, et al. Colocalization of hyperpolarization-activated, cyclic nucleotide-gated channel

subunits in rat retinal ganglion cells. *J Comp Neurol*. 2011; 519:2546–2573.

5. Knop GC, Seeliger MW, Thiel F, et al. Light responses in the mouse retina are prolonged upon targeted deletion of the HCN1 channel gene. *Eur J Neurosci*. 2008;28:2221–2230.
6. Ludwig A, Zong X, Jeglitsch M, Hofmann F, Biel M. A family of hyperpolarization-activated mammalian cation channels. *Nature*. 1998;393:587–591.
7. Gauss R, Seifert R, Kaupp UB. Molecular identification of a hyperpolarization-activated channel in sea urchin sperm. *Nature*. 1998;393:583–587.
8. Fain GL, Quandt FN, Bastian BL, Gerschenfeld HM. Contribution of a caesium-sensitive conductance increase to the rod photoresponse. *Nature*. 1978;272:466–469.
9. Bader CR, Macleish PR, Schwartz EA. A voltage-clamp study of the light response in solitary rods of the tiger salamander. *J Physiol*. 1979;296:1–26.
10. Baylor DA, Matthews G, Nunn BJ. Location and function of voltage-sensitive conductances in retinal rods of the salamander, *Ambystoma tigrinum*. *J Physiol*. 1984;354:203–223.
11. Hestrin S. The properties and function of inward rectification in rod photoreceptors of the tiger salamander. *J Physiol*. 1987;390:319–333.
12. Demontis GC, Longoni B, Barcaro U, Cervetto L. Properties and functional roles of hyperpolarization-gated currents in guinea-pig retinal rods. *J Physiol*. 1999;515:813–828.
13. Gargini C, Demontis GC, Bisti S, Cervetto L. Effects of blocking the hyperpolarization-activated current (Ih) on the cat electroretinogram. *Vision Res*. 1999;39:1767–1774.
14. Larsson HP. How is the heart rate regulated in the sinoatrial node? Another piece to the puzzle. *J Gen Physiol*. 2010;136: 237–241.
15. Tardif JC, Ford I, Tendera M, Bourassa MG, Fox K; for the INITIATIVE Investigators. Efficacy of ivabradine, a new selective I(f) inhibitor, compared with atenolol in patients with chronic stable angina. *Eur Heart J*. 2005;26:2529–2536.
16. Sulfi S, Timmis AD. Ivabradine - the first selective sinus node I(f) channel inhibitor in the treatment of stable angina. *Int J Clin Pract*. 2006;60:222–228.
17. Bucchi A, Barbuti A, Baruscotti M, DiFrancesco D. Heart rate reduction via selective 'funny' channel blockers. *Curr Opin Pharmacol*. 2007;7:208–213.
18. Borer JS, Tardif JC. Efficacy of ivabradine, a selective I(f) inhibitor, in patients with chronic stable angina pectoris and diabetes mellitus. *Am J Cardiol*. 2010;105:29–35.
19. Cervetto L, Demontis GC, Gargini C. Cellular mechanisms underlying the pharmacological induction of phosphenes. *Br J Pharmacol*. 2007;150:383–390.
20. Demontis GC, Gargini C, Paoli TG, Cervetto L. Selective Hcn1 channels inhibition by ivabradine in mouse rod photoreceptors. *Invest Ophthalmol Vis Sci*. 2009;50:1948–1955.
21. Della Santina L, Piano I, Cangiano L, et al. Processing of retinal signals in normal and HCN deficient mice. *PLoS One*. 2012;7: e29812.
22. Barrow AJ, Wu SM. Low-conductance HCN1 ion channels augment the frequency response of rod and cone photoreceptors. *J Neurosci*. 2009;29:5841–5853.
23. Della Santina L, Bouly M, Asta A, Demontis GC, Cervetto L, Gargini C. Effect of HCN channel inhibition on retinal morphology and function in normal and dystrophic rodents. *Invest Ophthalmol Vis Sci*. 2010;51:1016–1023.
24. Seeliger MW, Brombas A, Weiler R, et al. Modulation of rod photoreceptor output by HCN1 channels is essential for regular mesopic cone vision. *Nat Commun*. 2011;2:532.
25. Borer JS, Fox K, Jaillon P, Lerebours G; for the Ivabradine Investigators Group. Antianginal and antiischemic effects of ivabradine, an I(f) inhibitor, in stable angina: a randomized, double-blind, multicentered, placebo-controlled trial. *Circulation*. 2003;107:817–823.
26. Ragueneau I, Laveille C, Jochemsen R, Resplandy G, Funck-Brentano C, Jaillon P. Pharmacokinetic-pharmacodynamic modeling of the effects of ivabradine, a direct sinus node inhibitor, on heart rate in healthy volunteers. *Clin Pharmacol Ther*. 1998;64:192–203.
27. Pouzat C, Mazor O, Laurent G. Using noise signature to optimize spike-sorting and to assess neuronal classification quality. *J Neurosci Methods*. 2002;122:43–57.
28. Nikonov SS, Kholodenko R, Lem J, Pugh EN Jr. Physiological features of the S- and M-cone photoreceptors of wild-type mice from single-cell recordings. *J Gen Physiol*. 2006;127: 359–374.
29. Naarendorp F, Esdaille TM, Banden SM, Andrews-Labenski J, Gross OP, Pugh EN Jr. Dark light, rod saturation, and the absolute and incremental sensitivity of mouse cone vision. *J Neurosci*. 2010;30:12495–12507.
30. Chichilnisky EJ. A simple white noise analysis of neuronal light responses. *Network*. 2001;12:199–213.
31. Wang YV, Weick M, Demb JB. Spectral and temporal sensitivity of cone-mediated responses in mouse retinal ganglion cells. *J Neurosci*. 2011;31:7670–7681.
32. Zaghloul KA, Manookin MB, Borghuis BG, Boahen K, Demb JB. Functional circuitry for peripheral suppression in mammalian Y-type retinal ganglion cells. *J Neurophysiol*. 2007;97: 4327–4340.
33. Garvert MM, Gollisch T. Local and global contrast adaptation in retinal ganglion cells. *Neuron*. 2013;77:915–928.
34. Jones TA, Leake PA, Snyder RL, Stakhovskaya O, Bonham B. Spontaneous discharge patterns in cochlear spiral ganglion cells before the onset of hearing in cats. *J Neurophysiol*. 2007;98:1898–1908.
35. Bucchi A, Baruscotti M, DiFrancesco D. Current-dependent block of rabbit sino-atrial node I(f) channels by ivabradine. *J Gen Physiol*. 2002;120:1–13.
36. Bucchi A, Tognati A, Milanesi R, Baruscotti M, DiFrancesco D. Properties of ivabradine-induced block of HCN1 and HCN4 pacemaker channels. *J Physiol*. 2006;572:335–346.
37. Ozuysal Y, Baccus SA. Linking the computational structure of variance adaptation to biophysical mechanisms. *Neuron*. 2012;73:1002–1015.
38. Liu JK, Gollisch T. Spike-triggered covariance analysis reveals phenomenological diversity of contrast adaptation in the retina. *PLoS Comput Biol*. 2015;11:e1004425.
39. Cangiano L, Gargini C, Della Santina L, Demontis GC, Cervetto L. High-pass filtering of input signals by the Ih current in a non-spiking neuron, the retinal rod bipolar cell. *PLoS One*. 2007;2:e1327.
40. Barlow HB, Levick WR. Changes in the maintained discharge with adaptation level in the cat retina. *J Physiol*. 1969;202: 699–718.
41. Geffen MN, de Vries SE, Meister M. Retinal ganglion cells can rapidly change polarity from Off to On. *PLoS Biol*. 2007;5: e65.
42. Gollisch T, Meister M. Modeling convergent ON and OFF pathways in the early visual system. *Biol Cybern*. 2008;99: 263–278.
43. Gollisch T. Features and functions of nonlinear spatial integration by retinal ganglion cells. *J Physiol Paris*. 2013; 107:338–348.
44. Schwartz GW, Okawa H, Dunn FA, et al. The spatial structure of a nonlinear receptive field. *Nat Neurosci*. 2012;15:1572–1580.

Investigative Ophthalmology & Visual Science

45. Hochstein S, Shapley RM. Linear and nonlinear spatial subunits in Y cat retinal ganglion cells. *J Physiol*. 1976;262: 265–284.
46. Demb JB, Singer JH. Functional circuitry of the retina. *Annu Rev Vis Sci*. 2015;1:263–289.
47. Demb JB. Functional circuitry of visual adaptation in the retina. *J Physiol*. 2008;586:4377–4384.
48. Jarsky T, Cembrowski M, Logan SM, et al. A synaptic mechanism for retinal adaptation to luminance and contrast. *J Neurosci*. 2011;31:11003–11015.
49. Burrone J, Lagnado L. Synaptic depression and the kinetics of exocytosis in retinal bipolar cells. *J Neurosci*. 2000;20:568–578.
50. Bölinger D, Gollisch T. Closed-loop measurements of iso-response stimuli reveal dynamic nonlinear stimulus integration in the retina. *Neuron*. 2012;73:333–346.
51. Demb JB, Zaghloul K, Haarsma L, Sterling P. Bipolar cells contribute to nonlinear spatial summation in the brisk-transient (Y) ganglion cell in mammalian retina. *J Neurosci*. 2001;21:7447–7454.
52. Molnar A, Hsueh HA, Roska B, Werblin FS. Crossover inhibition in the retina: circuitry that compensates for nonlinear rectifying synaptic transmission. *J Comput Neurosci*. 2009;27:569–590.
53. Borghuis BG, Marvin JS, Looger LL, Demb JB. Two-photon imaging of nonlinear glutamate release dynamics at bipolar cell synapses in the mouse retina. *J Neurosci*. 2013;33:10972–10985.
54. Margolis DJ, Detwiler PB. Different mechanisms generate maintained activity in ON and OFF retinal ganglion cells. *J Neurosci*. 2007;27:5994–6005.
55. Thollon C, Cambarrat C, Vian J, Prost JF, Peglion JL, Vilaine JP. Electrophysiological effects of S 16257, a novel sino-atrial node modulator, on rabbit and guinea-pig cardiac preparations: comparison with UL-FS 49. *Br J Pharmacol*. 1994;112: 37–42.
56. Bois P, Bescond J, Renaudon B, Lenfant J. Mode of action of bradycardic agent, S 16257, on ionic currents of rabbit sinoatrial node cells. *Br J Pharmacol*. 1996;118:1051–1057.
57. Gardiner SM, Kemp PA, March JE, Bennett T. Acute and chronic cardiac and regional haemodynamic effects of the novel bradycardic agent, S16257, in conscious rats. *Br J Pharmacol*. 1995;115:579–586.
58. Colin P, Ghaleb B, Monnet X, et al. Contributions of heart rate and contractility to myocardial oxygen balance during exercise. *Am J Physiol Heart Circ Physiol*. 2003;284:H676–H682.
59. Colin P, Ghaleb B, Monnet X, Hittinger L, Berdeaux A. Effect of graded heart rate reduction with ivabradine on myocardial oxygen consumption and diastolic time in exercising dogs. *J Pharmacol Exp Ther*. 2004;308:236–240.
60. Fox K, Ford I, Steg PG, et al. Relationship between ivabradine treatment and cardiovascular outcomes in patients with stable coronary artery disease and left ventricular systolic dysfunction with limiting angina: a subgroup analysis of the randomized, controlled BEAUTIFUL trial. *Eur Heart J*. 2009; 30:2337–2345.
61. Field GD, Rieke F. Nonlinear signal transfer from mouse rods to bipolar cells and implications for visual sensitivity. *Neuron*. 2002;34:773–785.
62. Berntson A, Smith RG, Taylor WR. Transmission of single photon signals through a binary synapse in the mammalian retina. *Vis Neurosci*. 2004;21:693–702.
63. Tikidji-Hamburyan A, Reinhard K, Seitter H, et al. Retinal output changes qualitatively with every change in ambient illuminance. *Nat Neurosci*. 2015;18:66–74.
64. Brozoski TJ, Bauer CA, Caspary DM. Elevated fusiform cell activity in the dorsal cochlear nucleus of chinchillas with psychophysical evidence of tinnitus. *J Neurosci*. 2002;22: 2383–2390.
65. Kaltenbach JA, Rachel JD, Mathog TA, Zhang J, Falzarano PR, Lewandowski M. Cisplatin-induced hyperactivity in the dorsal cochlear nucleus and its relation to outer hair cell loss: relevance to tinnitus. *J Neurophysiol*. 2002;88:699–714.
66. Ali Z, Ringkamp M, Hartke TV, et al. Uninjured C-fiber nociceptors develop spontaneous activity and alpha-adrenergic sensitivity following L6 spinal nerve ligation in monkey. *J Neurophysiol*. 1999;81:455–466.
67. Wu G, Ringkamp M, Hartke TV, et al. Early onset of spontaneous activity in uninjured C-fiber nociceptors after injury to neighboring nerve fibers. *J Neurosci*. 2001;21: RC140.

Investigative Ophthalmology & Visual Science